Axion DM Search with Vector Boson Fusion

A. Gurrola[1], **E. Sheridan**[1], B. Soubasis[1]

Vanderbilt University[1]

May 12, 2020

Table of Contents

1. Project Introduction
2. Samples and Simulation
3. Event Selection Criteria
4. Final Thoughts

Motivating Axions

Motivating Axions

Theoretical Origins

- The structure of quantum chromodynamics permits a violation of the combined charge conjugation-parity symmetry, but experimental constraints (stemming from symmetry breaking repercussions on the neutron electric dipole moment) require this violation to be small
- It is unclear why this symmetry violation should simultaneously exist and be so small: this is the **strong CP problem**
- Roberto Peccei and Helen Quinn addressed this conundrum in 1977 by promoting the CP violation phase $\overline{\Theta}$—previously a Standard Model input requiring experimental measurement–to a scalar field which spontaneously breaks a new global symmetry (a Peccei–Quinn symmetry)
- The quanta (or boson) of this new scalar field is the **axion**

Motivating Axions

Theoretical Origins

- The structure of quantum chromodynamics permits a violation of the combined charge conjugation-parity symmetry, but experimental constraints (stemming from symmetry breaking repercussions on the neutron electric dipole moment) require this violation to be small
- It is unclear why this symmetry violation should simultaneously exist and be so small: this is the **strong CP problem**
- Roberto Peccei and Helen Quinn addressed this conundrum in 1977 by promoting the CP violation phase $\overline{\Theta}$—previously a Standard Model input requiring experimental measurement–to a scalar field which spontaneously breaks a new global symmetry (a Peccei–Quinn symmetry)
- The quanta (or boson) of this new scalar field is the **axion**

Axion Properties

- The axion is a neutral spin-0 boson, and different models permit widely varied mass values
- If the axion is sufficiently light, it presents itself as a dark matter candidate particle
- Axion theories require minor modifications to classical electrodynamics, as the presence of the axion serves to "rotate" the electric and magnetic fields into each other to an extent proportional to axion coupling and field strength

Motivating Axions

Theoretical Origins

- The structure of quantum chromodynamics permits a violation of the combined charge conjugation-parity symmetry, but experimental constraints (stemming from symmetry breaking repercussions on the neutron electric dipole moment) require this violation to be small
- It is unclear why this symmetry violation should simultaneously exist and be so small: this is the **strong CP problem**
- Roberto Peccei and Helen Quinn addressed this conundrum in 1977 by promoting the CP violation phase $\overline{\Theta}$—previously a Standard Model input requiring experimental measurement–to a scalar field which spontaneously breaks a new global symmetry (a Peccei–Quinn symmetry)
- The quanta (or boson) of this new scalar field is the **axion**

Axion Properties

- The axion is a neutral spin-0 boson, and different models permit widely varied mass values
- If the axion is sufficiently light, it presents itself as a dark matter candidate particle
- Axion theories require minor modifications to classical electrodynamics, as the presence of the axion serves to "rotate" the electric and magnetic fields into each other to an extent proportional to axion coupling and field strength

Axion Literature

- Astrophysics/cosmological experiments place bounds on axions and axion-like particles (ALPs) masses in some models, requiring them to be eV scale or lighter
- However, there still exist models which enable axions and ALPs to have masses in the MeV and GeV scales
- "Heavy axions" have been studied at the LHC, but primarily at higher mass scales due to sensitivity limitations

Motivating the Vector Boson Fusion Approach

Motivating the Vector Boson Fusion Approach

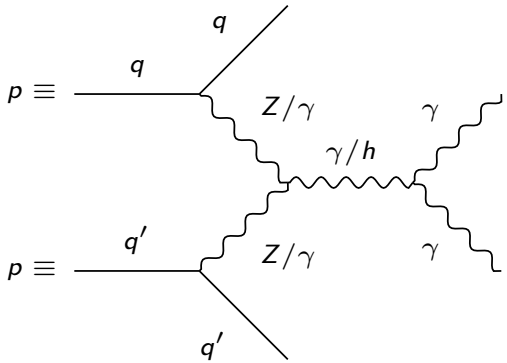

Motivating the Vector Boson Fusion Approach

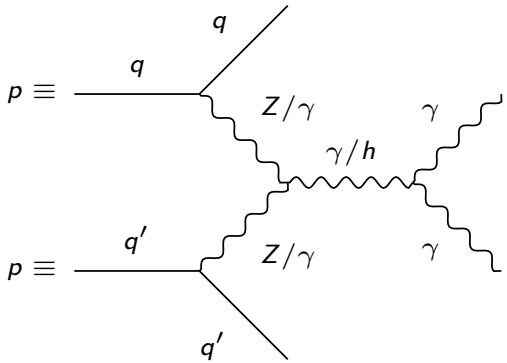

Description

- Vector boson fusion processes (VBF; exhibited above) are experimentally important due to their distinctiveness at the LHC
- In particular, the so-called "tagged jets" (the outgoing quarks in the above diagram) carry tell-tale high pseudorapidities
- This VBF kinematic signature suppresses background
- VBF cross sections typically surpass those of other topologies (Drell-Yan, etc) in new-physics processes with heavy new particles

Signal Generation

Signal Generation

Process

Signal generated using **MadGraph** (version **2.6.5**).

```
import model ALP_chiral_UFO
generate p p > ax j j QCD=0, ax > a a
```

We choose to consider an axion mass of **1 MeV**. Only default MadGraph cuts employed: e.g., $p_T^j > 20$ GeV, $p_T^\gamma > 10$ GeV

Signal Generation

Process

Signal generated using **MadGraph** (version **2.6.5**).

```
import model ALP_chiral_UFO
generate p p > ax j j QCD=0, ax > a a
```

We choose to consider an axion mass of **1 MeV**. Only default MadGraph cuts employed: e.g., $p_T^j > 20$ GeV, $p_T^\gamma > 10$ GeV

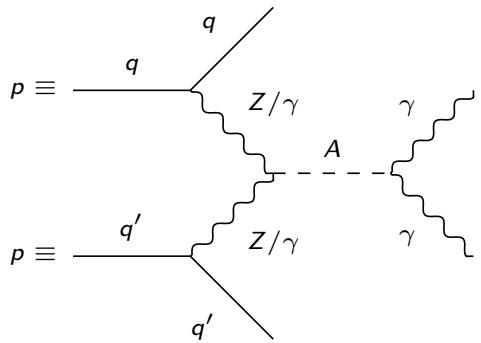

Signal Generation

Process

Signal generated using **MadGraph** (version **2.6.5**).

```
import model ALP_chiral_UFO
generate p p > ax j j QCD=0, ax > a a
```

We choose to consider an axion mass of **1 MeV**. Only default MadGraph cuts employed: e.g., $p_T^j > 20$ GeV, $p_T^\gamma > 10$ GeV

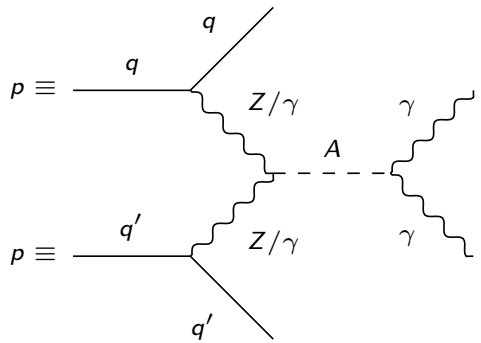

Comments

- `QCD = 0` selected due to our interest in axions with **negligible strong force couplings**
- `ax > a a` channel selected due to our emphasis on **lighter axions** (photons dominating heavier bosons)
- The significance of our studies arises in part from small axion mass scales probed

Initial Kinematics

Initial Kinematics

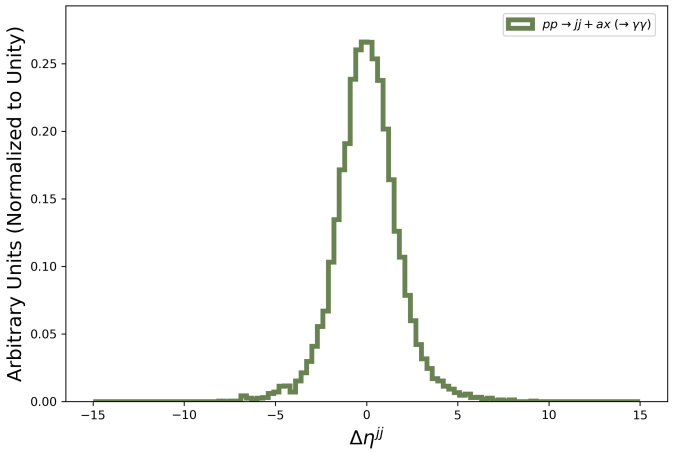

Initial Kinematics

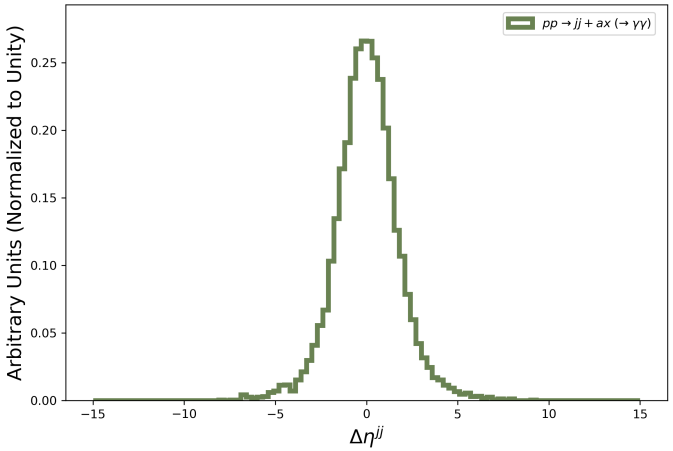

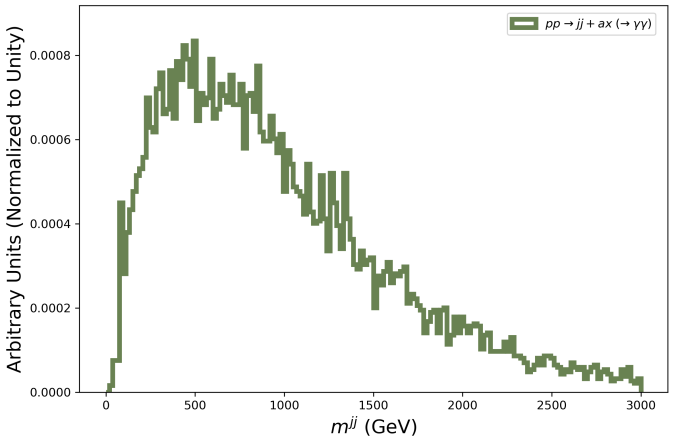

Initial Kinematics

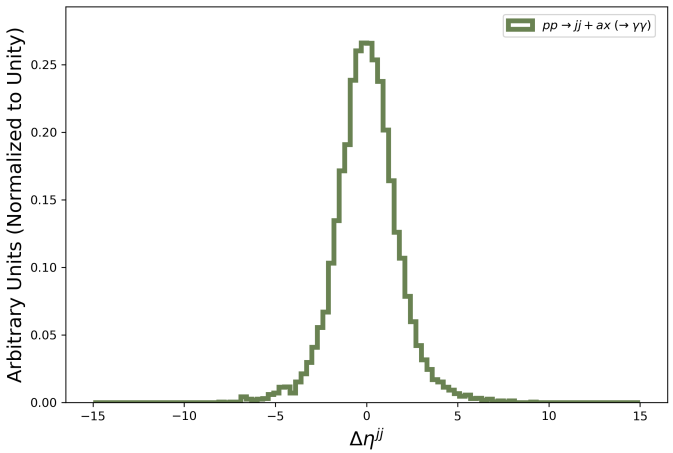

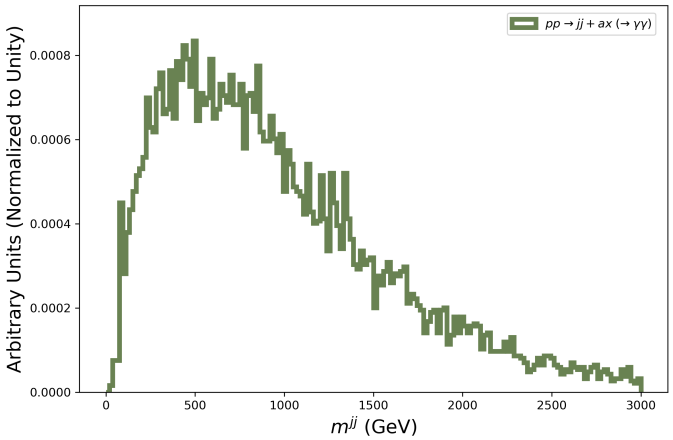

Comments

- Total cross section for signal is 0.786 $\pm$ 0.001 pb
- VBF processes are characterized by high $|\Delta\eta^{jj}|$, so a peak at 0 indicates that other processes dominate
- An m^{jj} peak at approx. 80-90 GeV indicates dominating `Z/W+/W- > j j` processes

Channel	Cross-Section (pb)
`g g > ax g g`	0.731 $\pm$ 1e-3
`u d > ax u d`	0.02414 $\pm$ 2e-4
`u u > ax u u`	0.01549 $\pm$ 6e-5

- Channel with next highest cross section on order of 1 fb.
- `q q > ax q q` processes can take on a VBF topology, but the `g g > ax g g` channel does not
- Despite the higher cross section, we avoid gluon-gluon processes due to their extensive prior analysis in the axion conext
- Additionally, gluon-gluon approaches are insensitive to light axions

Increasing VBF Purity in Signal

Increasing VBF Purity in Signal

Objective

- Want to generate signal events in a phase space region which emphasizes our eventual optimization (ensuring sufficient statistics)
- Equivalently, want to generate signal events primarily with the particular topologies (VBF) we will later select
- Thus before comparing with background, want to impose **MadGraph-level cuts** on signal events
- We select two topologies to try and minimize with such cuts: `g g > ax g g` and `Z > j j`

Increasing VBF Purity in Signal

Objective

- Want to generate signal events in a phase space region which emphasizes our eventual optimization (ensuring sufficient statistics)
- Equivalently, want to generate signal events primarily with the particular topologies (VBF) we will later select
- Thus before comparing with background, want to impose **MadGraph-level cuts** on signal events
- We select two topologies to try and minimize with such cuts: `g g > ax g g` and `Z > j j`

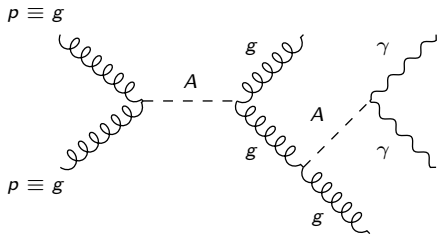

Increasing VBF Purity in Signal

Objective

- Want to generate signal events in a phase space region which emphasizes our eventual optimization (ensuring sufficient statistics)
- Equivalently, want to generate signal events primarily with the particular topologies (VBF) we will later select
- Thus before comparing with background, want to impose **MadGraph-level cuts** on signal events
- We select two topologies to try and minimize with such cuts: `g g > ax g g` and `Z > j j`

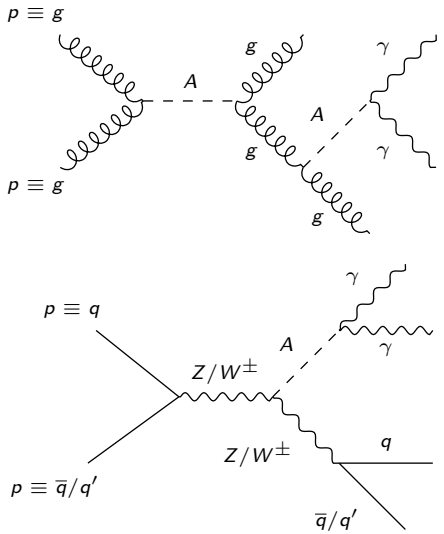

Increasing VBF Purity in Signal

Objective

- Want to generate signal events in a phase space region which emphasizes our eventual optimization (ensuring sufficient statistics)
- Equivalently, want to generate signal events primarily with the particular topologies (VBF) we will later select
- Thus before comparing with background, want to impose **MadGraph-level cuts** on signal events
- We select two topologies to try and minimize with such cuts: `g g > ax g g` and `Z > j j`

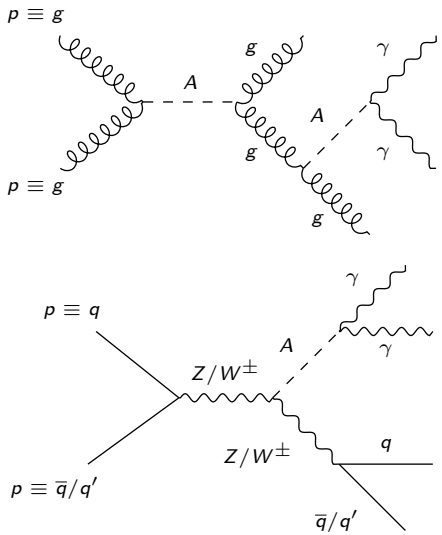

Final Approach

Choose to generate 1000000 signal events with all of the previous commands/setting, along with the following additional MadGraph selections.
$|\Delta\eta^{jj}| > 2.4$, $m^{jj} > 120$ GeV

- The gluon-gluon channel exhibits predominately low $|\Delta\eta^{jj}|$, so we apply a cut with the hopes of reducing its cross section
- The vector boson resonance channel satisfies $m^{jj} \approx 80$ GeV, so we apply an m^{jj} cut with the hopes of also reducing that cross section

The cross section for this signal is 0.10235 $\pm$ 2.82e-5 pb, and the following breakdown of individual channel cross-sections gives a first indication of our success. While the gluon-gluon channel still dominates, we've achieved a VBF signal purity sufficient to achieve the necessary statistics during optimization.

Increasing VBF Purity in Signal

Objective

- Want to generate signal events in a phase space region which emphasizes our eventual optimization (ensuring sufficient statistics)
- Equivalently, want to generate signal events primarily with the particular topologies (VBF) we will later select
- Thus before comparing with background, want to impose **MadGraph-level cuts** on signal events
- We select two topologies to try and minimize with such cuts: `g g > ax g g` and `Z > j j`

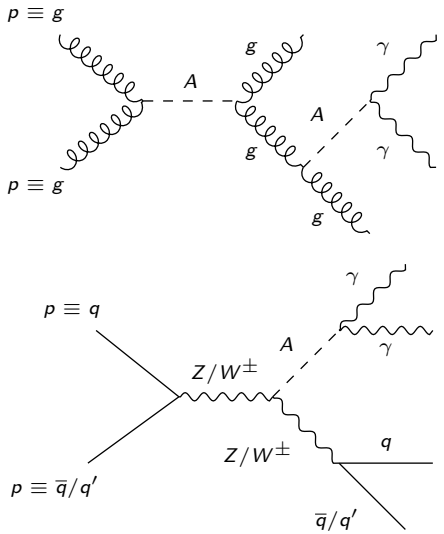

Final Approach

Choose to generate 1000000 signal events with all of the previous commands/setting, along with the following additional MadGraph selections.
$|\Delta\eta^{jj}| > 2.4$, $m^{jj} > 120$ GeV

- The gluon-gluon channel exhibits predominately low $|\Delta\eta^{jj}|$, so we apply a cut with the hopes of reducing its cross section
- The vector boson resonance channel satisfies $m^{jj} \approx 80$ GeV, so we apply an m^{jj} cut with the hopes of also reducing that cross section

The cross section for this signal is 0.10235 $\pm$ 2.82e-5 pb, and the following breakdown of individual channel cross-sections gives a first indication of our success. While the gluon-gluon channel still dominates, we've achieved a VBF signal purity sufficient to achieve the necessary statistics during optimization.

Channel	Cross-Section (pb)
`g g > ax g g`	0.06911 $\pm$ 2.28e-5
VBF channel	0.03324 $\pm$ 5.1e-5

Background Generation

Background Generation

Process

We're interested in comparing our signal with **two** background processes. First, a general dijet, diphoton channel which we generate as follows.

```
generate p p > j j a a
```

Second, a more specific, VBF-oriented background with no QCD vertices, mimicking our signal generation.

```
generate p p > j j a a QCD=0
```

Recognizing that during optimization we will be selecting events with high momentum (VBF jets being boosted by the heavy vector boson production), for both background processes we generate events in H_T bins. In particular, we sought to simulate 1000000 events per background process per each of the following bins (all values given in GeV).

$[0, 100]$, $[100, 200]$, $[200, 400]$, $[400, 600]$, $[600, 800]$,
$[800, 1200]$, $[1200, 1600]$, $[1600, \infty)$

We note that MadGraph was unable to produce the full million events for higher H_T bins (likely due to diagram complexity), but a sufficient number of events to reach desired optimization statistics was still achieved.

Prototypical Feynman diagrams are given for the general (top) and QCD $= 0$ (bottom) cases.

Background Generation

Process

We're interested in comparing our signal with **two** background processes. First, a general dijet, diphoton channel which we generate as follows.

```
generate p p > j j a a
```

Second, a more specific, VBF-oriented background with no QCD vertices, mimicking our signal generation.

```
generate p p > j j a a QCD=0
```

Recognizing that during optimization we will be selecting events with high momentum (VBF jets being boosted by the heavy vector boson production), for both background processes we generate events in H_T bins. In particular, we sought to simulate 1000000 events per background process per each of the following bins (all values given in GeV).

$[0, 100]$, $[100, 200]$, $[200, 400]$, $[400, 600]$, $[600, 800]$,
$[800, 1200]$, $[1200, 1600]$, $[1600, \infty)$

We note that MadGraph was unable to produce the full million events for higher H_T bins (likely due to diagram complexity), but a sufficient number of events to reach desired optimization statistics was still achieved.

Prototypical Feynman diagrams are given for the general (top) and QCD $= 0$ (bottom) cases.

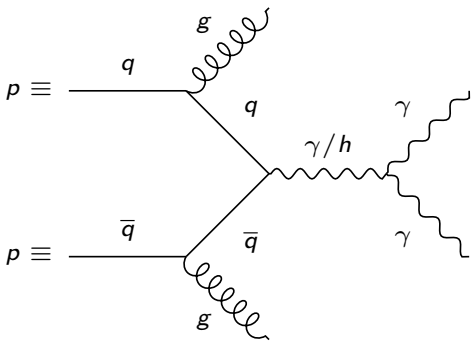

Background Generation

Process

We're interested in comparing our signal with **two** background processes. First, a general dijet, diphoton channel which we generate as follows.

```
generate p p > j j a a
```

Second, a more specific, VBF-oriented background with no QCD vertices, mimicking our signal generation.

```
generate p p > j j a a QCD=0
```

Recognizing that during optimization we will be selecting events with high momentum (VBF jets being boosted by the heavy vector boson production), for both background processes we generate events in H_T bins. In particular, we sought to simulate 1000000 events per background process per each of the following bins (all values given in GeV).

$[0, 100]$, $[100, 200]$, $[200, 400]$, $[400, 600]$, $[600, 800]$,
$[800, 1200]$, $[1200, 1600]$, $[1600, \infty)$

We note that MadGraph was unable to produce the full million events for higher H_T bins (likely due to diagram complexity), but a sufficient number of events to reach desired optimization statistics was still achieved.

Prototypical Feynman diagrams are given for the general (top) and QCD $= 0$ (bottom) cases.

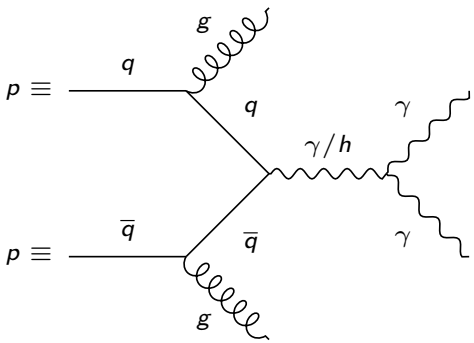

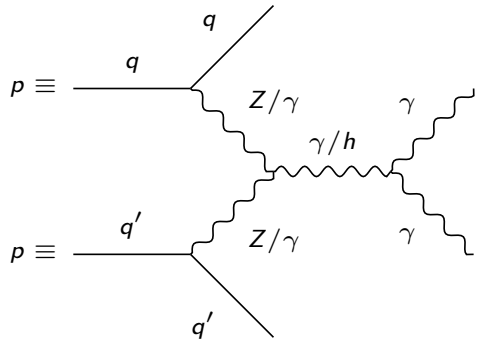

Kinematics with MG-Level Cuts

Kinematics with MG-Level Cuts

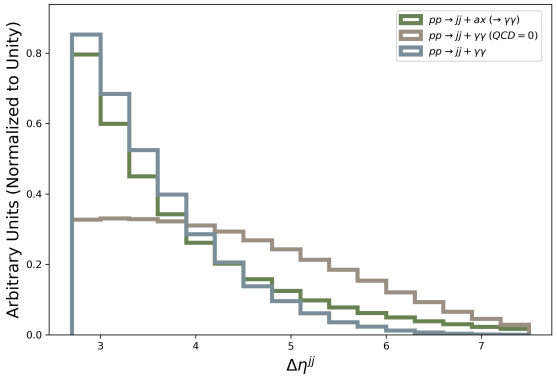

Kinematics with MG-Level Cuts

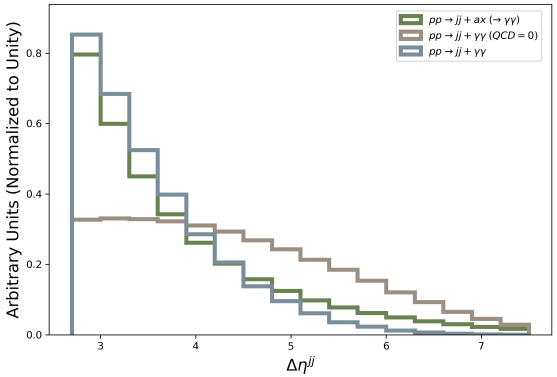

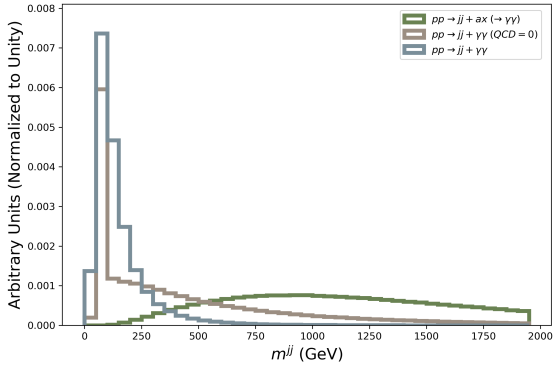

Kinematics with MG-Level Cuts

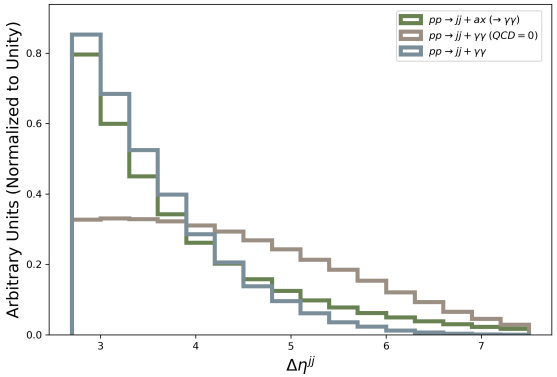

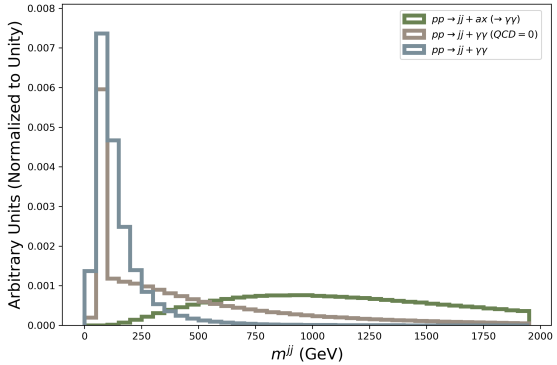

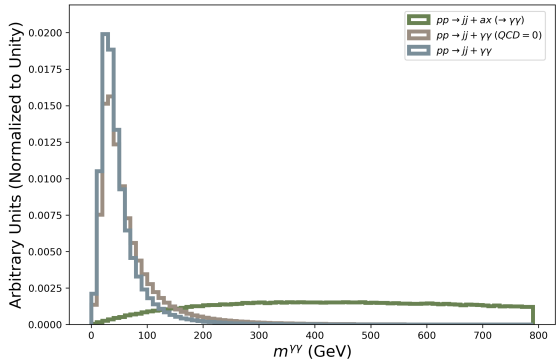

Kinematics with MG-Level Cuts

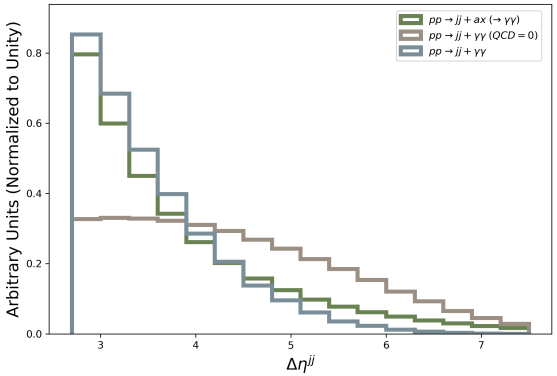

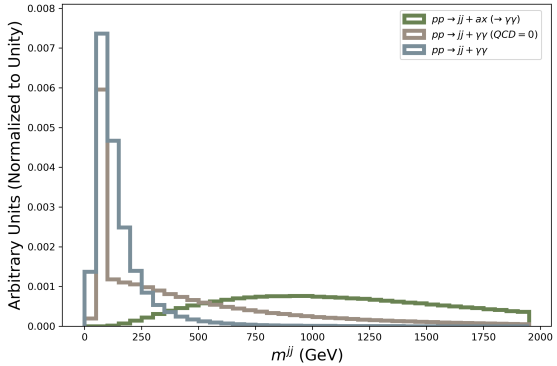

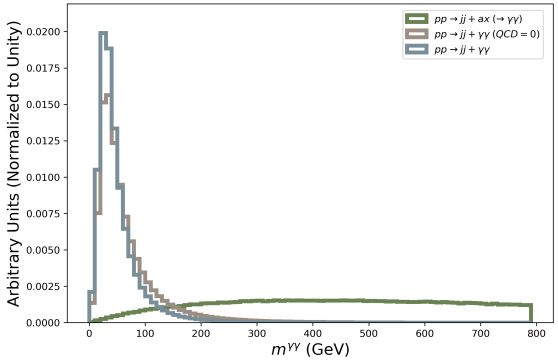

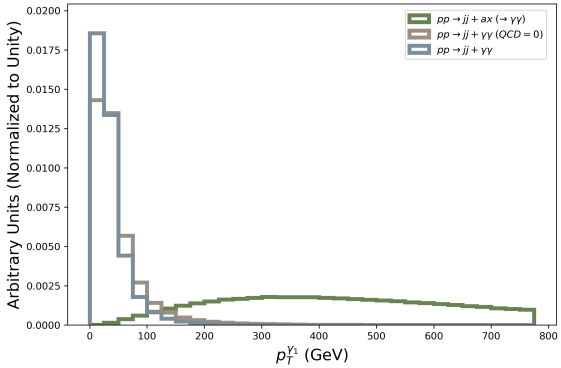

Kinematics with MG-Level Cuts

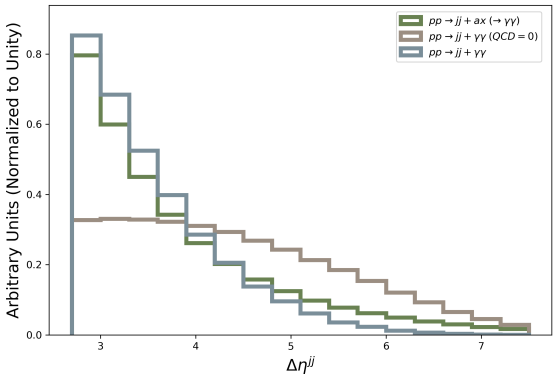

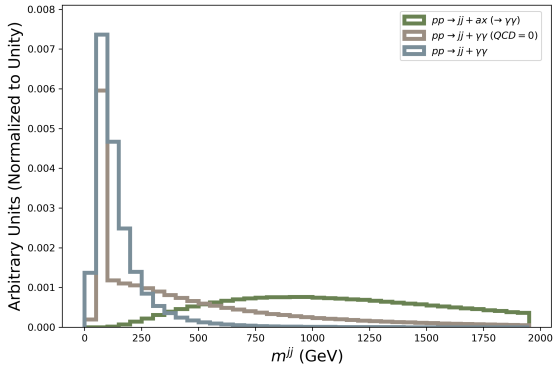

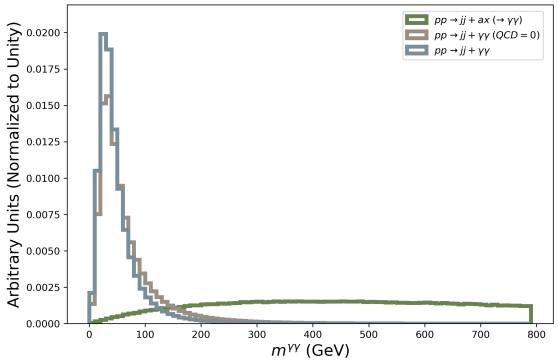

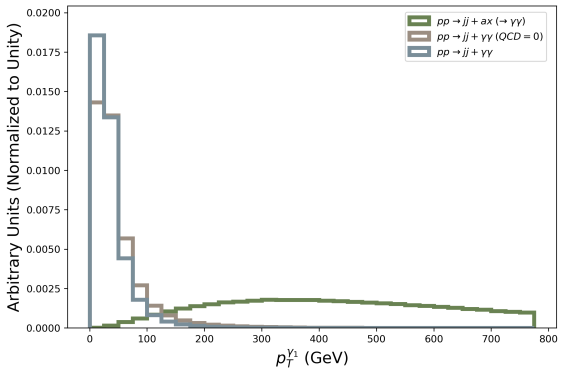

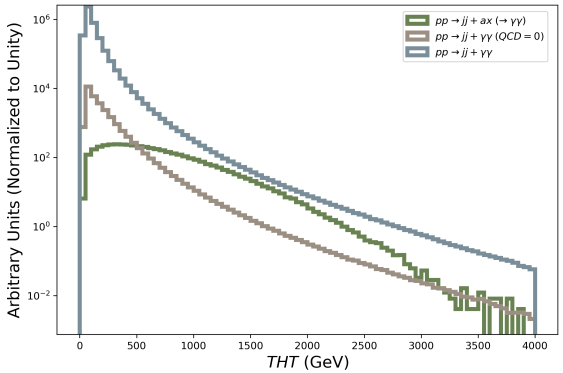

Kinematics with MG-Level Cuts

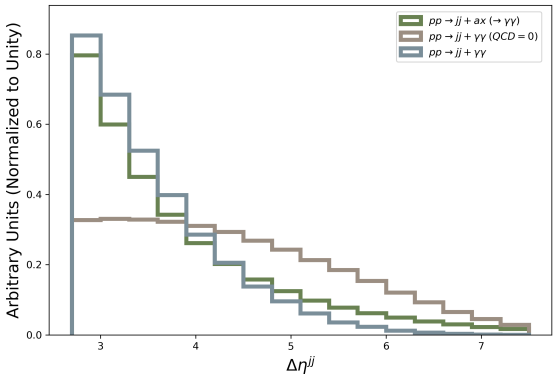

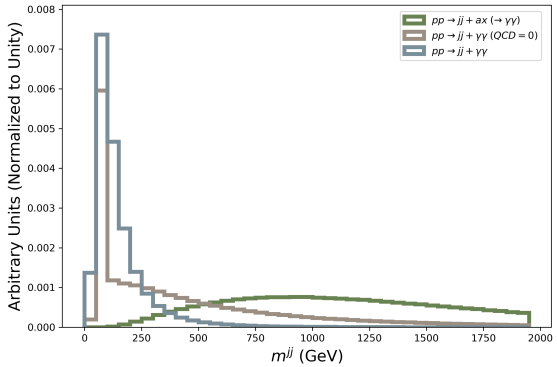

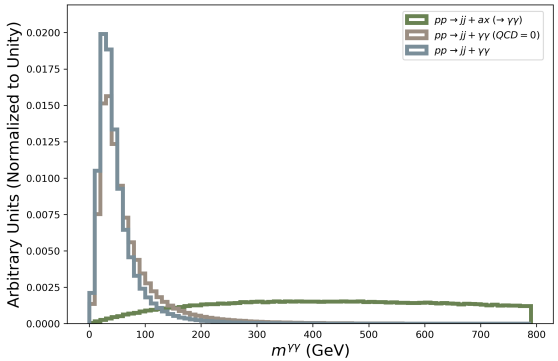

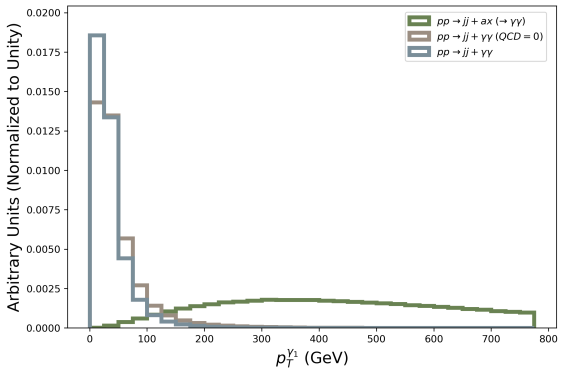

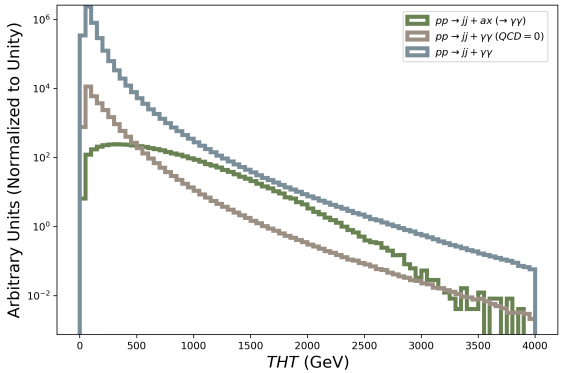

Comments

The first four kinematic plots exhibit high signal-background discriminating power in the following kinematic variables.

$\Delta\eta^{jj}$, m^{jj}, $m^{\gamma\gamma}$, p_T^{γ}

This is a little more subtle in the $\Delta\eta^{jj}$ case, but the VBF subset of our signal has higher $\Delta\eta^{jj}$ so cuts in this variable will boost significance. These plots motivate our optimization. The final kinematic plot demonstrates how our H_T-binned background samples are "stiched" together smoothly (noise occurring only at the higher end of our final H_T bin).

Jet Variable Selection Optimization ($\Delta\eta^{jj}$, m^{jj})

Jet Variable Selection Optimization ($\Delta\eta^{jj}$, m^{jj})

Process

We begin by optimizing the $\Delta\eta^{jj}$ and m^{jj} selections simultaneously (to account for correlations). We perform a gridsearch on pairs of selections of the form $|\Delta\eta^{jj}| > \eta_0$, $m^{jj} > m_0^j$ on the following values (m^{jj} given in GeV).

$(\eta_0, m_0^j) \in \{2.6, 3.1, 3.6, 4.1, 4.6, 5.1, 5.6, 6.1\} \times \{120, 500, 750, 1000, 1250, 1500, 1750, 2000\}$

We compute significance in two ways on each of these $8 \cdot 8 = 64$ scenarios: without (left) and with (right) a systematic uncertainty term. To avoid divergences arising from low background yield, we alter the base significance form $\frac{S}{B}$ to $\frac{S}{\sqrt{S+B}}$ and implement a systematic uncertainty approximation with the modification $S/\sqrt{S+B+(r\cdot B)^2}$ for $r \in [0,1]$

Jet Variable Selection Optimization ($\Delta\eta^{jj}$, m^{jj})

Process

We begin by optimizing the $\Delta\eta^{jj}$ and m^{jj} selections simultaneously (to account for correlations). We perform a gridsearch on pairs of selections of the form $|\Delta\eta^{jj}| > \eta_0$, $m^{jj} > m_0^j$ on the following values (m^{jj} given in GeV).

$(\eta_0, m_0^j) \in \{2.6, 3.1, 3.6, 4.1, 4.6, 5.1, 5.6, 6.1\} \times \{120, 500, 750, 1000, 1250, 1500, 1750, 2000\}$

We compute significance in two ways on each of these $8 \cdot 8 = 64$ scenarios: without (left) and with (right) a systematic uncertainty term. To avoid divergences arising from low background yield, we alter the base significance form $\frac{S}{B}$ to $\frac{S}{\sqrt{S+B}}$ and implement a systematic uncertainty approximation with the modification $S/\sqrt{S+B+(r\cdot B)^2}$ for $r \in [0,1]$

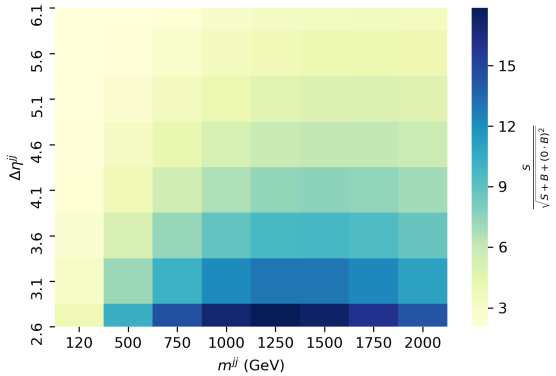

Jet Variable Selection Optimization ($\Delta\eta^{jj}$, m^{jj})

Process

We begin by optimizing the $\Delta\eta^{jj}$ and m^{jj} selections simultaneously (to account for correlations). We perform a gridsearch on pairs of selections of the form $|\Delta\eta^{jj}| > \eta_0$, $m^{jj} > m_0^j$ on the following values (m^{jj} given in GeV).

$(\eta_0, m_0^j) \in \{2.6, 3.1, 3.6, 4.1, 4.6, 5.1, 5.6, 6.1\} \times \{120, 500, 750, 1000, 1250, 1500, 1750, 2000\}$

We compute significance in two ways on each of these $8 \cdot 8 = 64$ scenarios: without (left) and with (right) a systematic uncertainty term. To avoid divergences arising from low background yield, we alter the base significance form $\frac{S}{B}$ to $\frac{S}{\sqrt{S+B}}$ and implement a systematic uncertainty approximation with the modification $S/\sqrt{S+B+(r\cdot B)^2}$ for $r \in [0,1]$

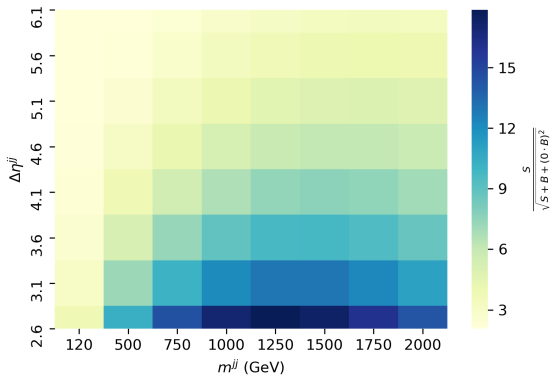

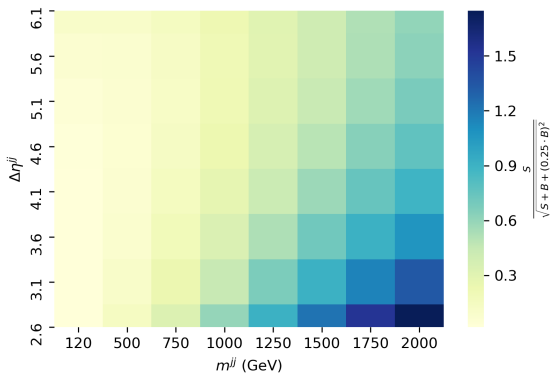

Conclusions

Experimental constraints motivate prioritization of higher $\Delta\eta^{jj}$ cuts, and our approximation of sys. uncert. fails at higher m^{jj} cuts. Thus, we invoke the non-sys. uncert. results and pursue two selection pairs: a tight (lower significance/more experimental feasibility) cut $(\eta_0, m_0^j) = (3.6, 1250)$ and a loose (higher significance/less experimental feasibility) cut $(\eta_0, m_0^j) = (2.6, 1250)$.

Checking Photon Discriminating Power

Checking Photon Discriminating Power

Confirmation

Before proceeding to the optimization for the other two variables—$m^{\gamma\gamma}$, p_T^{γ}—we quickly check that our tight/loose $\Delta\eta^{jj}$, m^{jj} cuts haven't reduced discriminating power. We consider kinematic plots in the tight cuts scenario.

Checking Photon Discriminating Power

Confirmation

Before proceeding to the optimization for the other two variables—$m^{\gamma\gamma}$, p_T^{γ}—we quickly check that our tight/loose $\Delta\eta^{jj}$, m^{jj} cuts haven't reduced discriminating power. We consider kinematic plots in the tight cuts scenario.

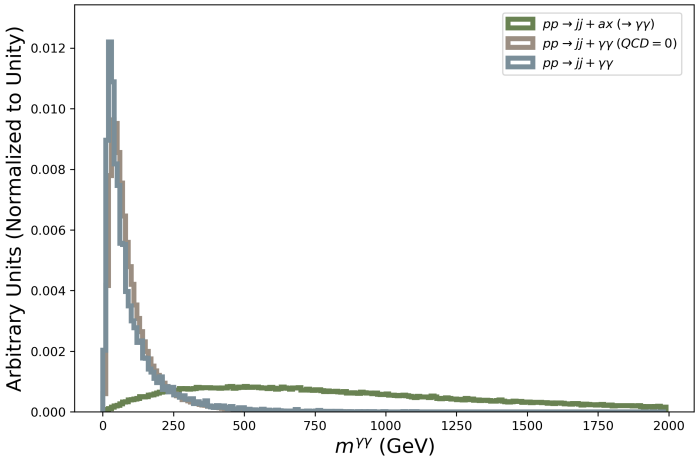

Checking Photon Discriminating Power

Confirmation

Before proceeding to the optimization for the other two variables—$m^{\gamma\gamma}$, p_T^{γ}—we quickly check that our tight/loose $\Delta\eta^{jj}$, m^{jj} cuts haven't reduced discriminating power. We consider kinematic plots in the tight cuts scenario.

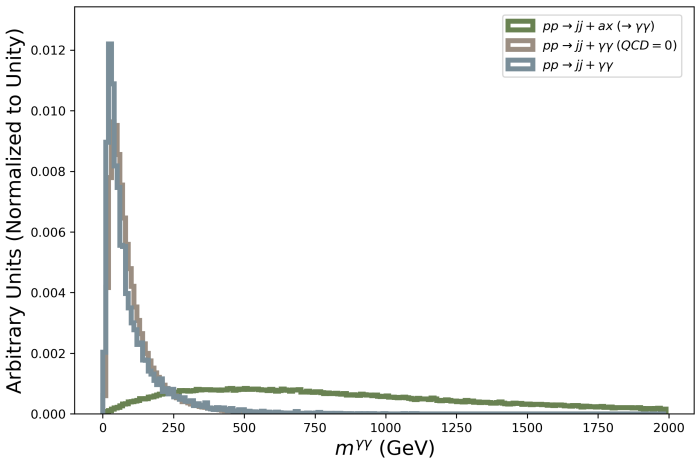

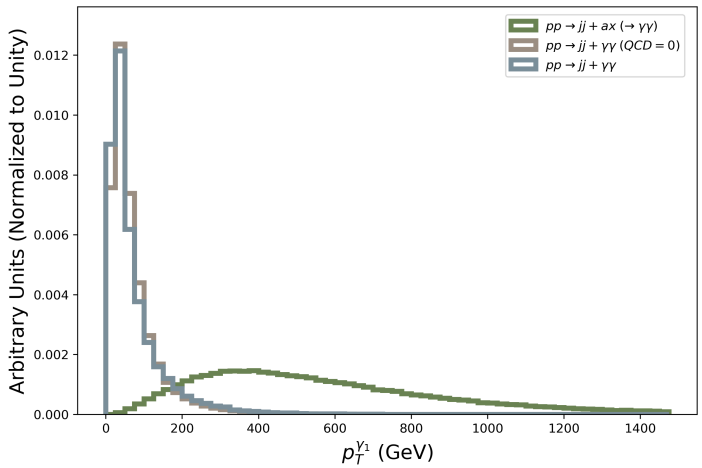

Conclusions

Our discriminating power has been preserved (these plots behave similarly in the loose cuts scenario), allowing us to continue on to a photon kinematics optimization routine.

Photon Variable Selection Optimization ($m^{\gamma\gamma}$, p_T^{γ})

Photon Variable Selection Optimization ($m^{\gamma\gamma}$, p_T^{γ})

Process

We now optimize the $m^{\gamma\gamma}$ and p_T^{γ} selections simultaneously, performing a gridsearch on pairs of selections of the form $m^{\gamma\gamma} > m_0^{\gamma}$, $p_T^{\gamma} > \gamma_0$ on the following values (both variables given in GeV).

$(m_0^{\gamma}, \gamma_0) \in \{200, 250, 300, 350, 400, 450, 500, 550, 600, 650, 700\} \times \{100, 150, 200, 250, 300, 350, 400, 450, 500\}$

We compute significance in two ways on each of these $11 \cdot 9 = 99$ scenarios–in particular, using different systematic uncertainty coefficients–for both the tight (left two plots) and loose (right two plots) jet kinematic selections.

Photon Variable Selection Optimization ($m^{\gamma\gamma}$, p_T^{γ})

Process

We now optimize the $m^{\gamma\gamma}$ and p_T^{γ} selections simultaneously, performing a gridsearch on pairs of selections of the form $m^{\gamma\gamma} > m_0^{\gamma}$, $p_T^{\gamma} > \gamma_0$ on the following values (both variables given in GeV).

$(m_0^{\gamma}, \gamma_0) \in \{200, 250, 300, 350, 400, 450, 500, 550, 600, 650, 700\} \times \{100, 150, 200, 250, 300, 350, 400, 450, 500\}$

We compute significance in two ways on each of these $11 \cdot 9 = 99$ scenarios–in particular, using different systematic uncertainty coefficients–for both the tight (left two plots) and loose (right two plots) jet kinematic selections.

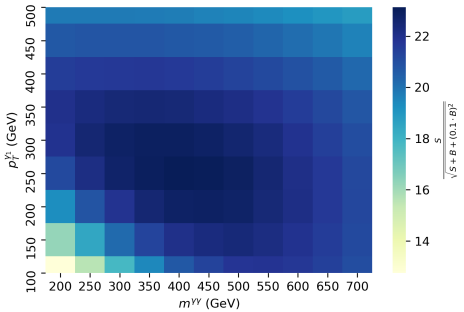

Photon Variable Selection Optimization ($m^{\gamma\gamma}$, p_T^{γ})

Process

We now optimize the $m^{\gamma\gamma}$ and p_T^{γ} selections simultaneously, performing a gridsearch on pairs of selections of the form $m^{\gamma\gamma} > m_0^{\gamma}$, $p_T^{\gamma} > \gamma_0$ on the following values (both variables given in GeV).

$(m_0^{\gamma}, \gamma_0) \in \{200, 250, 300, 350, 400, 450, 500, 550, 600, 650, 700\} \times \{100, 150, 200, 250, 300, 350, 400, 450, 500\}$

We compute significance in two ways on each of these $11 \cdot 9 = 99$ scenarios–in particular, using different systematic uncertainty coefficients–for both the tight (left two plots) and loose (right two plots) jet kinematic selections.

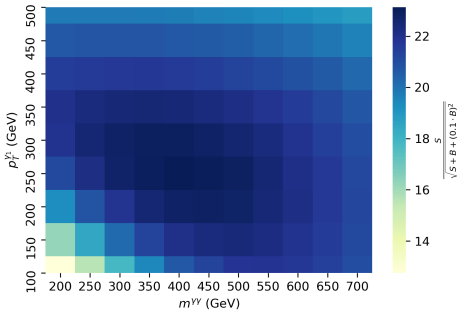

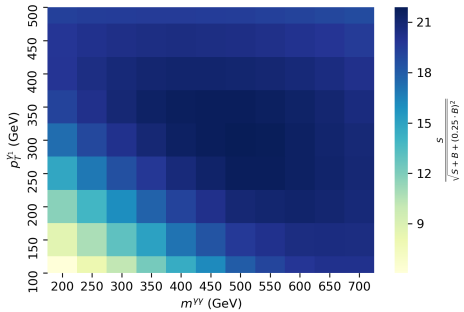

Photon Variable Selection Optimization ($m^{\gamma\gamma}$, p_T^{γ})

Process

We now optimize the $m^{\gamma\gamma}$ and p_T^{γ} selections simultaneously, performing a gridsearch on pairs of selections of the form $m^{\gamma\gamma} > m_0^{\gamma}$, $p_T^{\gamma} > \gamma_0$ on the following values (both variables given in GeV).

$(m_0^{\gamma}, \gamma_0) \in \{200, 250, 300, 350, 400, 450, 500, 550, 600, 650, 700\} \times \{100, 150, 200, 250, 300, 350, 400, 450, 500\}$

We compute significance in two ways on each of these $11 \cdot 9 = 99$ scenarios–in particular, using different systematic uncertainty coefficients–for both the tight (left two plots) and loose (right two plots) jet kinematic selections.

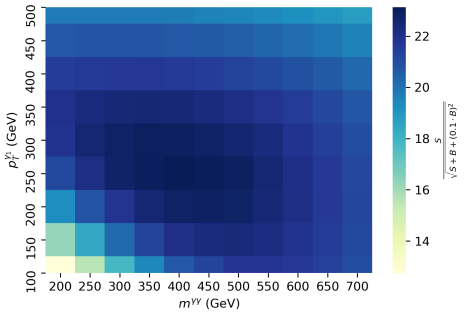

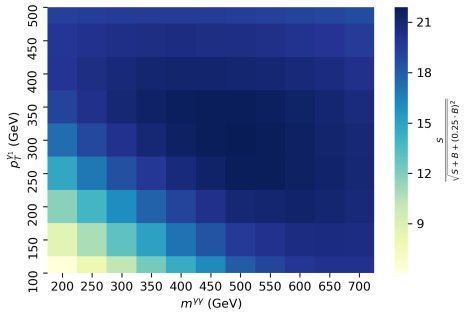

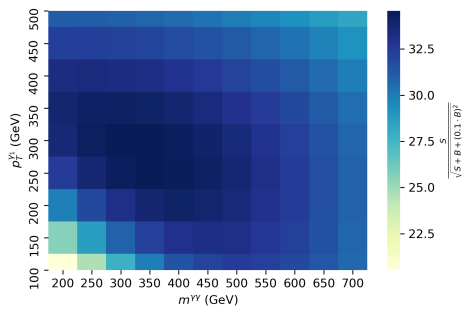

Photon Variable Selection Optimization ($m^{\gamma\gamma}$, p_T^{γ})

Process

We now optimize the $m^{\gamma\gamma}$ and p_T^{γ} selections simultaneously, performing a gridsearch on pairs of selections of the form $m^{\gamma\gamma} > m_0^{\gamma}$, $p_T^{\gamma} > \gamma_0$ on the following values (both variables given in GeV).

$(m_0^{\gamma}, \gamma_0) \in \{200, 250, 300, 350, 400, 450, 500, 550, 600, 650, 700\} \times \{100, 150, 200, 250, 300, 350, 400, 450, 500\}$

We compute significance in two ways on each of these $11 \cdot 9 = 99$ scenarios–in particular, using different systematic uncertainty coefficients–for both the tight (left two plots) and loose (right two plots) jet kinematic selections.

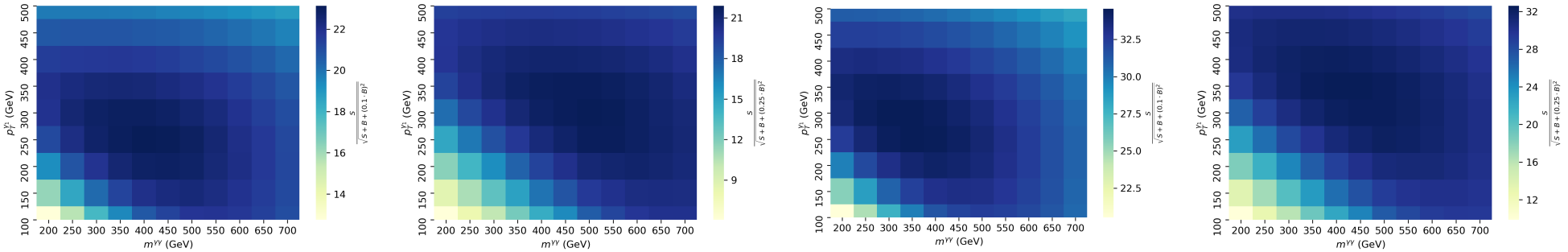

Conclusions

Each heatmap provides us with a slightly different local maxima for significance: we therefore decide to pursue four (m_0^{γ}, γ_0) selections (ordering coinciding with the heatmap ordering).

$(m_0^{\gamma}, \gamma_0) \in \{(400, 250), (500, 300), (350, 250), (400, 350)\}$

Jet Variable Selection Optimization, Again ($\Delta\eta^{jj}$, m^{jj})

Jet Variable Selection Optimization, Again ($\Delta\eta^{jj}$, m^{jj})

Process

Given our four pairs of $m^{\gamma\gamma}$, p_T^{γ} selections, we now return to the jet kinematic variables to explore significance in the $\Delta\eta^{jj}$, m^{jj} phase space for each photon kinematics selection. This time, we perform a gridsearch on a smaller phase space region, with pairs of selections of the form $|\Delta\eta^{jj}| > \eta_0$, $m^{jj} > m_0^j$ on the following values (m^{jj} again given in GeV).

$(\eta_1, m_1^j) \in \{2.6, 3.1, 3.6, 4.1\} \times \{750, 1000, 1250, 1500, 1750, 2000\}$

We compute significance in just one way on each of these $4 \cdot 6 = 24$ scenarios, simply using the systematic uncertainty coefficient which led to the selection of that particular $m^{\gamma\gamma}$, p_T^{γ} selections. Our plots are then ordered as follows.

$(m_0^{\gamma}, \gamma_0) = (400, 250), (m_0^{\gamma}, \gamma_0) = (500, 300), (m_0^{\gamma}, \gamma_0) = (350, 250), (m_0^{\gamma}, \gamma_0) = (400, 350)$

Jet Variable Selection Optimization, Again ($\Delta\eta^{jj}$, m^{jj})

Process

Given our four pairs of $m^{\gamma\gamma}$, p_T^{γ} selections, we now return to the jet kinematic variables to explore significance in the $\Delta\eta^{jj}$, m^{jj} phase space for each photon kinematics selection. This time, we perform a gridsearch on a smaller phase space region, with pairs of selections of the form $|\Delta\eta^{jj}| > \eta_0$, $m^{jj} > m_0^j$ on the following values (m^{jj} again given in GeV).

$(\eta_1, m_1^j) \in \{2.6, 3.1, 3.6, 4.1\} \times \{750, 1000, 1250, 1500, 1750, 2000\}$

We compute significance in just one way on each of these $4 \cdot 6 = 24$ scenarios, simply using the systematic uncertainty coefficient which led to the selection of that particular $m^{\gamma\gamma}$, p_T^{γ} selections. Our plots are then ordered as follows.

$(m_0^{\gamma}, \gamma_0) = (400, 250), (m_0^{\gamma}, \gamma_0) = (500, 300), (m_0^{\gamma}, \gamma_0) = (350, 250), (m_0^{\gamma}, \gamma_0) = (400, 350)$

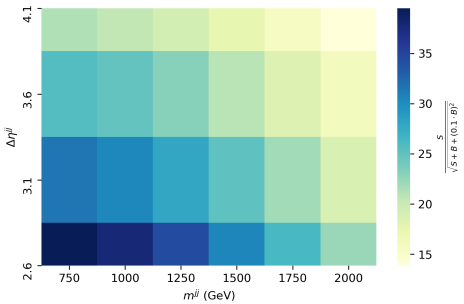

Jet Variable Selection Optimization, Again ($\Delta\eta^{jj}$, m^{jj})

Process

Given our four pairs of $m^{\gamma\gamma}$, p_T^{γ} selections, we now return to the jet kinematic variables to explore significance in the $\Delta\eta^{jj}$, m^{jj} phase space for each photon kinematics selection. This time, we perform a gridsearch on a smaller phase space region, with pairs of selections of the form $|\Delta\eta^{jj}| > \eta_0$, $m^{jj} > m_0^j$ on the following values (m^{jj} again given in GeV).

$(\eta_1, m_1^j) \in \{2.6, 3.1, 3.6, 4.1\} \times \{750, 1000, 1250, 1500, 1750, 2000\}$

We compute significance in just one way on each of these $4 \cdot 6 = 24$ scenarios, simply using the systematic uncertainty coefficient which led to the selection of that particular $m^{\gamma\gamma}$, p_T^{γ} selections. Our plots are then ordered as follows.

$(m_0^{\gamma}, \gamma_0) = (400, 250), (m_0^{\gamma}, \gamma_0) = (500, 300), (m_0^{\gamma}, \gamma_0) = (350, 250), (m_0^{\gamma}, \gamma_0) = (400, 350)$

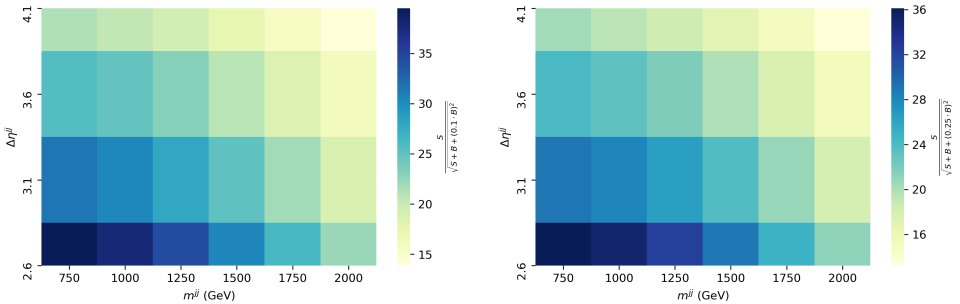

Jet Variable Selection Optimization, Again ($\Delta\eta^{jj}$, m^{jj})

Process

Given our four pairs of $m^{\gamma\gamma}$, p_T^{γ} selections, we now return to the jet kinematic variables to explore significance in the $\Delta\eta^{jj}$, m^{jj} phase space for each photon kinematics selection. This time, we perform a gridsearch on a smaller phase space region, with pairs of selections of the form $|\Delta\eta^{jj}| > \eta_0$, $m^{jj} > m_0^j$ on the following values (m^{jj} again given in GeV).

$(\eta_1, m_1^j) \in \{2.6, 3.1, 3.6, 4.1\} \times \{750, 1000, 1250, 1500, 1750, 2000\}$

We compute significance in just one way on each of these $4 \cdot 6 = 24$ scenarios, simply using the systematic uncertainty coefficient which led to the selection of that particular $m^{\gamma\gamma}$, p_T^{γ} selections. Our plots are then ordered as follows.

$(m_0^{\gamma}, \gamma_0) = (400, 250), (m_0^{\gamma}, \gamma_0) = (500, 300), (m_0^{\gamma}, \gamma_0) = (350, 250), (m_0^{\gamma}, \gamma_0) = (400, 350)$

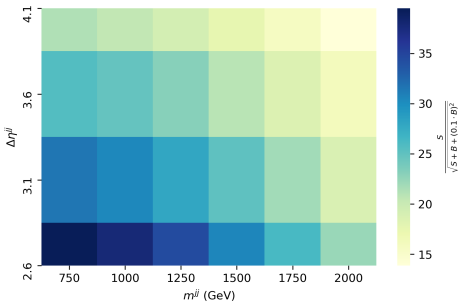

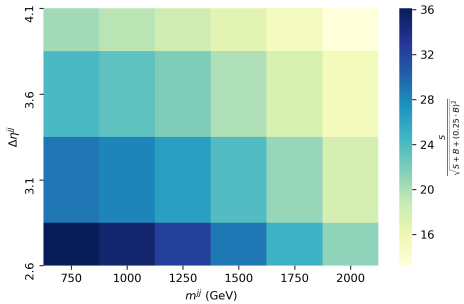

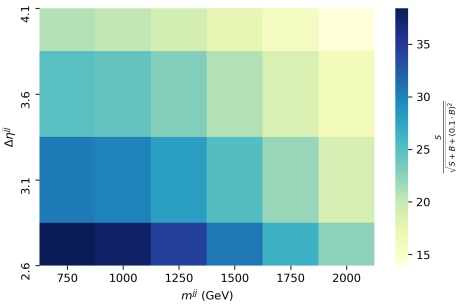

Jet Variable Selection Optimization, Again ($\Delta\eta^{jj}$, m^{jj})

Process

Given our four pairs of $m^{\gamma\gamma}$, p_T^{γ} selections, we now return to the jet kinematic variables to explore significance in the $\Delta\eta^{jj}$, m^{jj} phase space for each photon kinematics selection. This time, we perform a gridsearch on a smaller phase space region, with pairs of selections of the form $|\Delta\eta^{jj}| > \eta_0$, $m^{jj} > m_0^j$ on the following values (m^{jj} again given in GeV).

$(\eta_1, m_1^j) \in \{2.6, 3.1, 3.6, 4.1\} \times \{750, 1000, 1250, 1500, 1750, 2000\}$

We compute significance in just one way on each of these $4 \cdot 6 = 24$ scenarios, simply using the systematic uncertainty coefficient which led to the selection of that particular $m^{\gamma\gamma}$, p_T^{γ} selections. Our plots are then ordered as follows.

$(m_0^{\gamma}, \gamma_0) = (400, 250), (m_0^{\gamma}, \gamma_0) = (500, 300), (m_0^{\gamma}, \gamma_0) = (350, 250), (m_0^{\gamma}, \gamma_0) = (400, 350)$

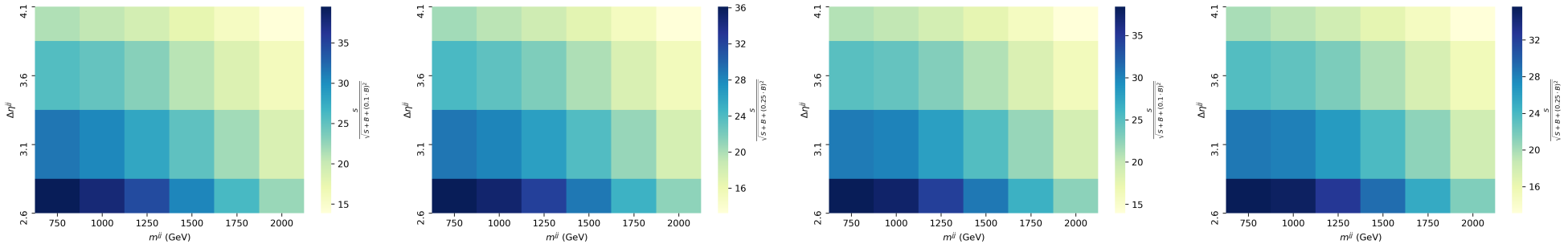

Conclusions

Our four scenarios exhibit an approximately uniform shape, with a maximum near $(\eta_1, m_1^j) = (2.6, 750)$. Once again, we consider high $\Delta\eta^{jj}$ selections to be more experimentally feasible. We also seek to incorporate a realistically high systematic uncertainty. These priorities motivate the following selections.

$|\Delta\eta^{jj}| > 3.6$, $m^{jj} > 750$, $m^{\gamma\gamma} > 500$, $p_T^{\gamma} > 300$

Selection Significance

Selection Significance

Objective

Given our new parameter selections, want to quickly summarize our progress.

- Want to compare signal-background kinematic plots normalized to cross section between before (below) and after (right, top) selections are made
- Want to examine how significance scales with luminosity for different significance metrics (right, bottom)

Selection Significance

Objective

Given our new parameter selections, want to quickly summarize our progress.

- Want to compare signal-background kinematic plots normalized to cross section between before (below) and after (right, top) selections are made
- Want to examine how significance scales with luminosity for different significance metrics (right, bottom)

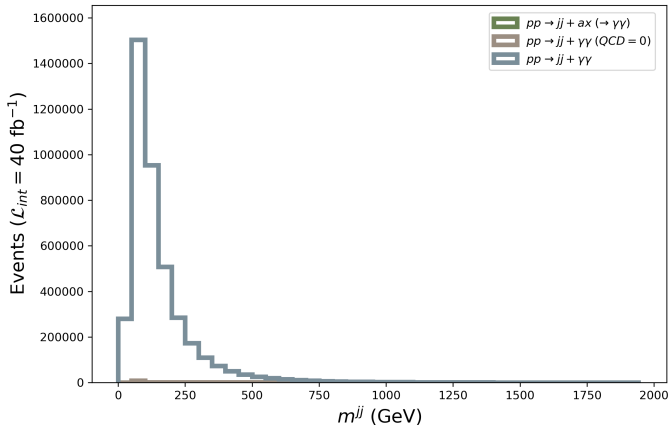

Selection Significance

Objective

Given our new parameter selections, want to quickly summarize our progress.

- Want to compare signal-background kinematic plots normalized to cross section between before (below) and after (right, top) selections are made
- Want to examine how significance scales with luminosity for different significance metrics (right, bottom)

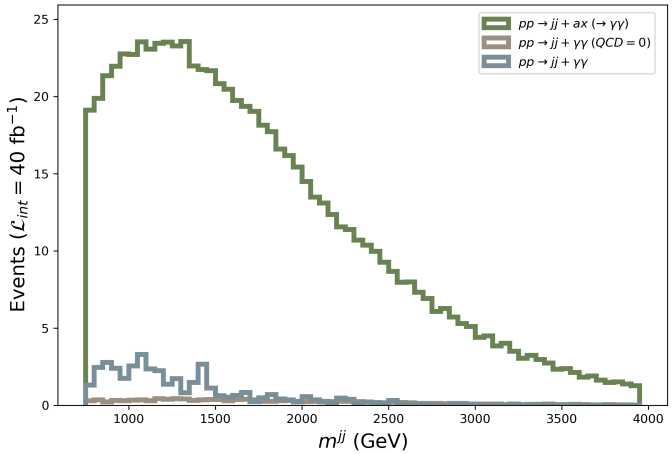

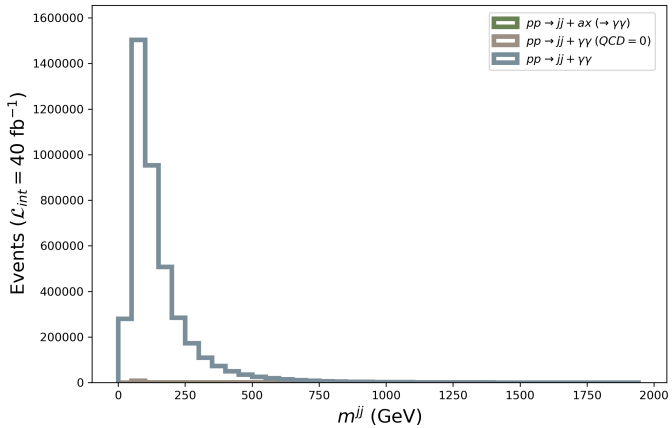

Selection Significance

Objective

Given our new parameter selections, want to quickly summarize our progress.

- Want to compare signal-background kinematic plots normalized to cross section between before (below) and after (right, top) selections are made
- Want to examine how significance scales with luminosity for different significance metrics (right, bottom)

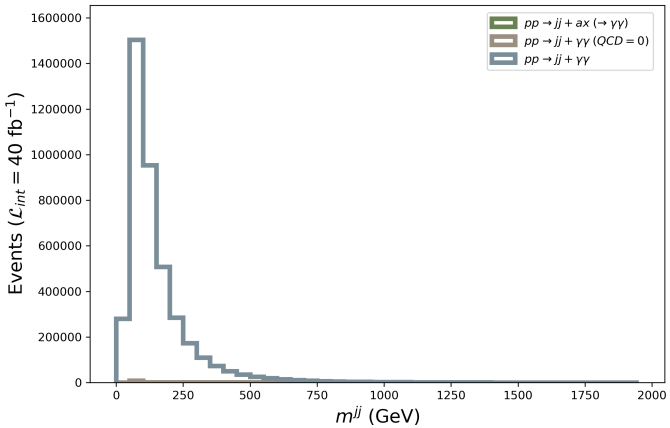

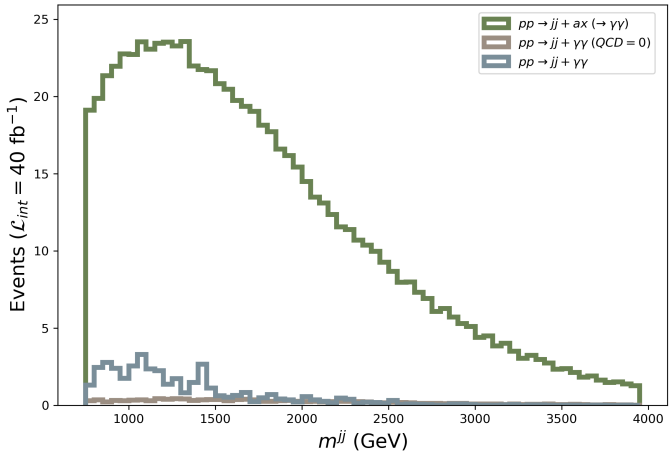

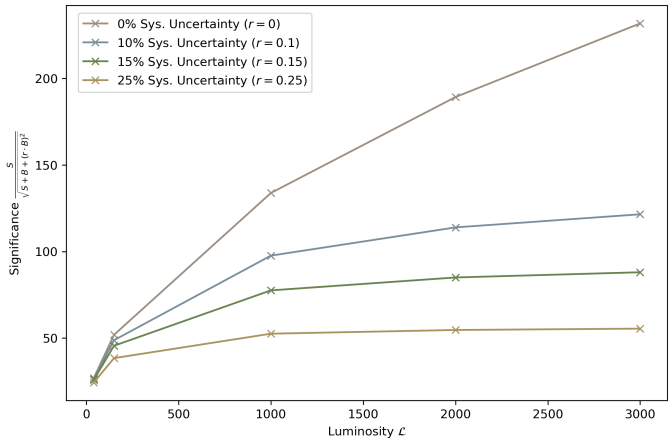

Conclusions

We've selected a region of phase space where our new physics processes dominate and discovery potential is high.

Final Thoughts

Final Thoughts

Summary

- Introduced the theory of our particular BSM interest–the axion–and the collider topology we plan to use to study it, vector boson fusion (VBF)
- Discussed our generation of signal events, including imposed MadGraph-level selections to increase VBF purity
- Examined our generation of background events, including the choice of two distinct background channels and our H_T binning process
- Analyzed kinematic variables and elaborated on our three-step selection optimization process on $\Delta\eta^{jj}$, m^{jj}, $m^{\gamma\gamma}$, p_T^j, eventually arriving at an experimentally and statistically motivated selection for each of these variable
- Investigated signal versus background yield and the significance associated with our four final selections

Final Thoughts

Summary

- Introduced the theory of our particular BSM interest–the axion–and the collider topology we plan to use to study it, vector boson fusion (VBF)
- Discussed our generation of signal events, including imposed MadGraph-level selections to increase VBF purity
- Examined our generation of background events, including the choice of two distinct background channels and our H_T binning process
- Analyzed kinematic variables and elaborated on our three-step selection optimization process on $\Delta\eta^{jj}$, m^{jj}, $m^{\gamma\gamma}$, p_T^j, eventually arriving at an experimentally and statistically motivated selection for each of these variable
- Investigated signal versus background yield and the significance associated with our four final selections

Next Steps

- Resolve technical issues (potentially relating to `ax > a a` decay) and study how our findings vary with axions of different masses
- Investigate why virtual axion processes dominate (thoughts?)
- Anything else?